Hillslope hydrologic connectivity controls riparian groundwater turnover: Implications of catchment structure for riparian buffering and stream water sources

Kelsey G. Jencso,[1] Brian L. McGlynn,[1] Michael N. Gooseff,[2] Kenneth E. Bencala,[3] and Steven M. Wondzell[4]

Received 27 October 2009; revised 7 March 2010; accepted 18 May 2010; published 15 October 2010.

[1] Hydrologic connectivity between catchment upland and near stream areas is essential for the transmission of water, solutes, and nutrients to streams. However, our current understanding of the role of riparian zones in mediating landscape hydrologic connectivity and the catchment scale export of water and solutes is limited. We tested the relationship between the duration of hillslope-riparian-stream (HRS) hydrologic connectivity and the rate and degree of riparian shallow groundwater turnover along four HRS well transects within a set of nested mountain catchments (Tenderfoot Creek Experimental Forest, MT). Transect HRS water table connectivity ranged from 9 to 123 days during the annual snowmelt hydrograph. Hillslope water was always characterized by low specific conductance (~27 μS cm^{-1}). In transects with transient hillslope water tables, riparian groundwater specific conductance was elevated during base flow conditions (~127 μS cm^{-1}) but shifted toward hillslope signatures once a HRS groundwater connection was established. The degree of riparian groundwater turnover was proportional to the duration of HRS connectivity and inversely related to the riparian: hillslope area ratios (buffer ratio; $r^2 = 0.95$). We applied this relationship to the stream network in seven subcatchments within the Tenderfoot Creek Experimental Forest and compared their turnover distributions to source water contributions measured at each catchment outlet. The amount of riparian groundwater exiting each of the seven catchments was linearly related ($r^2 = 0.92$) to their median riparian turnover time. Our observations suggest that the size and spatial arrangement of hillslope and riparian zones along a stream network and the timing and duration of groundwater connectivity between them is a first-order control on the magnitude and timing of water and solutes observed at the catchment outlet.

Citation: Jencso, K. G., B. L. McGlynn, M. N. Gooseff, K. E. Bencala, and S. M. Wondzell (2010), Hillslope hydrologic connectivity controls riparian groundwater turnover: Implications of catchment structure for riparian buffering and stream water sources, *Water Resour. Res.*, *46*, W10524, doi:10.1029/2009WR008818.

1. Introduction

[2] Hydrologic investigations have been conducted across a wide array of research catchments and have identified numerous controls on runoff generation, including topography [*Anderson and Burt*, 1978; *Beven*, 1978; *McGuire et al.*, 2005], soil distributions [*Buttle et al.*, 2004; *Soulsby et al.*, 2004; *Soulsby et al.*, 2006], and geology [*Shaman et al.*, 2004; *Uchida et al.*, 2005]. Landscape structure (topography and topology) can be particularly important for spatial patterns of water and solute movement in catchments with shallow soils. However, the relationship between variability in catchment structure and the timing, magnitude, and distribution of runoff and solute sources remains unclear. This lack of clarity is partially due to poor understanding of the role of riparian zones in mediating/buffering the upslope delivery of water and solutes across stream networks. We suggest that our understanding of catchment hydrology and biogeochemistry can be advanced through assessment of the dominant controls on hydrological connectivity among hillslope-riparian source areas and quantification of riparian buffering.

[3] Hydrologic connectivity between hillslope and riparian zones is typically transient but can occur when saturation develops across their interfaces [*Jencso et al.*, 2009]. Hillslope hydrologic connections to riparian zones may be largely controlled by topography in catchments with shallow soil and poorly permeable bedrock. Especially important is the convergence and divergence of catchment topography which controls the size of upslope accumulated area (UAA)

[1]Department of Land Resources and Environmental Sciences, Montana State University, Bozeman, Montana, USA.
[2]Civil Environmental Engineering Department, Penn State University, University Park, Pennsylvania, USA.
[3]U.S. Geological Survey, Menlo Park, California, USA.
[4]U.S. Forest Service, Pacific Northwest Research Station Olympia Forestry Sciences Lab, Olympia, Washington, USA.

0043-1397/10/2009WR008818

[*Anderson and Burt*, 1977; *Beven*, 1978]. Because of variability in topography within catchments, hillslope UAA sizes and therefore transient groundwater inputs to riparian zones can be spatially variable throughout the stream network [*Weyman*, 1970].

[4] *Jencso et al.* [2009] recently compared the duration of hillslope-riparian-stream (HRS) water table connectivity to hillslope UAA size. They found that the size of hillslope UAA was a first-order control on the duration of HRS shallow groundwater connectivity across 24 HRS landscape transitions ($r^2 = 0.91$). Larger hillslope sizes exhibited sustained connections to their riparian and stream zones, whereas more transient connections occurred across HRS sequences with smaller hillslope sizes. They applied this relationship to the entire stream network to quantify catchment scale hydrologic connectivity through time and found that the amount of the stream network's riparian zones that were connected to the uplands varied from 4% to 67% during the year.

[5] Because of their location between hillslopes and streams, riparian zones can modulate or buffer the delivery of water and solutes when hillslope connectivity is established across the stream network [*Hill*, 2000]. Research in headwater catchments has emphasized the importance of the riparian zone as a relatively restricted part of the catchment which can exert a disproportionately large influence on stream hydrologic and chemical response [*Mulholland*, 1992; *Brinson*, 1993; *Cirmo and McDonnell*, 1997]. The definitions of riparian buffering are diverse and often depend on the water quality or hydrologic process of interest. One use of the term refers to biogeochemical transformations [*Cirmo and McDonnell*, 1997] that often occur in near stream zones (e.g., redox reactions and denitrification). Another common use of the term refers to the volumetric buffering of upslope runoff by resident near stream groundwater [*McGlynn and McDonnell*, 2003b]. In the context of this study we focus on the volume buffering and source water mixing aspects of riparian function.

[6] Identifying spatial and temporal hydrologic connectivity among HRS zones can be an important step in understanding the evolution of stream solute and source water signatures during storm events. When a HRS connection is established, hillslope groundwater moves from the slope down through the adjacent riparian zone. Plot scale investigations have suggested that the mixing and displacement of riparian groundwater (turnover) by hillslope runoff is a first-order control on hillslope water [*McGlynn et al.*, 1999], solute [*McGlynn and McDonnell*, 2003b], and nutrient [*Burt et al.*, 1999; *Hill*, 2000; *Carlyle and Hill*, 2001; *McGlynn and McDonnell*, 2003a; *Ocampo et al.*, 2006; *Pacific et al.*, 2010] signatures expressed in streamflow. Source water separations at the catchment outlet [*Hooper et al.*, 1997; *Burns et al.*, 2001; *McGlynn and McDonnell*, 2003b] and theoretical exercises [*Chanat and Hornberger*, 2003; *McGlynn and Seibert*, 2003] have also suggested that the rate at which turnover occurs may be proportional to the size of the riparian zone and the timing, duration, or magnitude of hillslope hydrologic connectivity to the riparian zone.

[7] Information gleaned from individual plot or catchment scale tracer investigations have suggested hydrologic connectivity to the riparian zone as a factor in the timing of water and solute delivery to the stream. Despite these previous investigations a general conceptualization of how a stream's spatial sources of water change through an event remains elusive. Little field research to date has explored how HRS hydrologic connectivity frequency and duration relates to the turnover of water and solutes in the riparian zone, how riparian zones "buffer" hillslope connectivity, and how these dynamics are distributed across entire stream networks. This limits our ability to move forward and assess riparian buffering of hillslope groundwater connections in a whole catchment context.

[8] In this paper we combine landscape analysis of HRS connectivity [*Jencso et al.*, 2009] and riparian buffering [*McGlynn and Seibert*, 2003] with high-frequency, spatially distributed observations of HRS shallow groundwater connectivity (24 well transects; 146 wells) and solute dynamics (4 hillslope-riparian-stream transitions). We extrapolate these observations across seven stream networks with contrasting catchment structure and compare them with catchment-scale hillslope and riparian spatial source water separations during the annual snowmelt hydrograph to address the following questions:

[9] 1. What is the effect of HRS connectivity duration on the degree of turnover of water and solutes in riparian zones?

[10] 2. How does landscape structure influence stream network hydrologic dynamics and the timing and amount of source waters detected at the catchment outlet?

[11] We utilize a landscape analysis-based framework to link landscape-scale hydrologic and solute dynamics with their topographic/geomorphic controls and present a way to transfer these dynamics across stream networks and catchments of differing structure.

2. Site Description

[12] The Tenderfoot Creek Experimental Forest (TCEF) (latitude, 46°55′N, longitude, 110°52′W) is located in the Little Belt Mountains of the Lewis and Clark National Forest in Central Montana, USA (Figure 1). Tenderfoot Creek forms the headwaters of the Smith River, a tributary of the Missouri. The TCEF is an ideal site for ascertaining relationships between variability in landscape structure and catchment hydrochemical response because it is composed of seven gauged catchments with a range of topographic complexity, watershed shapes, and hillslope and riparian sizes.

[13] The seven TCEF subcatchments range in size from 3 to 22.8 km^2. In general,the catchment headwaters possess moderately sloping (average slope ~8°) extensive (up to 1200 m long) hillslopes and variable width riparian zones [*Jencso et al.*, 2009]. Flathead Sandstone and Wolsey Shale comprise the parent material in the upper portions of each catchment [*Farnes et al.*, 1995]. Approaching the main stem of Tenderfoot Creek the streams become more incised, hillslopes become shorter (<500 m) and steeper (average slope ~20°), and riparian areas are narrower than in the catchment headwaters [*Jencso et al.*, 2009]. Basement rocks of granite gneiss occur at lower elevations [*Farnes et al.*, 1995], and they are visible as exposed cliffs and talus slopes. All three rock strata in the TCEF are relatively impermeable with potential for deeper groundwater transmission along geologic contacts and fractures within the Wolsey shale [*Reynolds*, 1995].

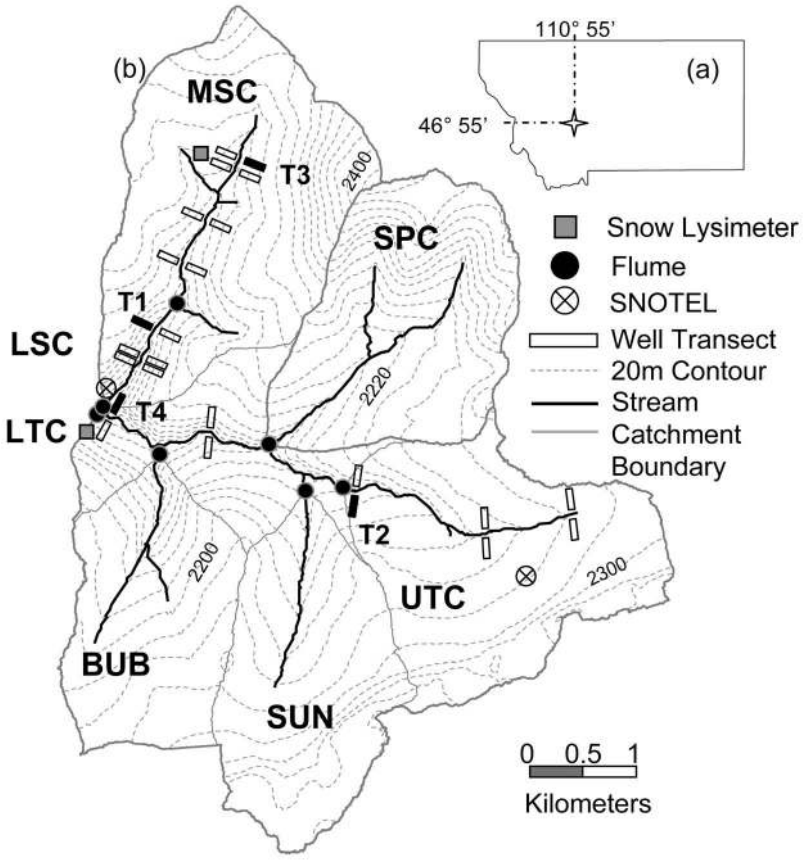

Figure 1. Site location and instrumentation of the TCEF catchment. (a) Catchment location in the Rocky Mountains, MT. (b) Catchment flumes, well transects, and SNOTEL instrumentation locations. Specific transects highlighted in this study are filled in black and labeled T1–T4. Transect extents are not drawn to scale.

[14] Soil depths are relatively consistent across hillslope (0.5–1.0 m) and riparian (1–2.0 m) zones with localized upland areas of deeper soils. The most extensive soil types in the TCEF are loamy skeletal, mixed Typic Cryochrepts located along hillslope positions and clayey, mixed Aquic Cryoboralfs in riparian zones and parks [*Holdorf*, 1981]. Riparian soils have high organic matter.

[15] The TCEF is a snowmelt dominated catchment. The 1961–1990 average annual precipitation is 840 mm [*Farnes et al.*, 1995]. Monthly precipitation generally peaks in December or January (100–120 mm per month) and declines to a late July through October dry period (45–55 mm per month). Approximately 75% of the annual precipitation falls during November through May, primarily as snow. Snowmelt and peak runoff typically occur in late May or early June. Lowest runoff occurs in the late summer through winter months.

3. Methods

3.1. Terrain Analysis

[16] The TCEF stream network, riparian area, hillslope area, and their buffer ratios were delineated using a 1 m Airborne Laser Swath Mapping digital elevation model (DEM) resampled to a 10 m grid cell size. Elevation measurements were achieved at a horizontal sampling interval of the order <1 m, with vertical accuracies of ±0.05 to ±0.15 m. We used the 10 m DEM to quantify each catchment's hillslope and riparian UAA sizes following DEM landscape analysis methods outlined by *McGlynn and Seibert* [2003].

[17] The area required for perennial stream flow (creek threshold initiation area) was estimated as 40 ha for Lower Tenderfoot Creek (LTC), Upper Tenderfoot Creek (UTC), Sun Creek (SUN), Spring Park Creek (SPC), Lower Stringer Creek (LSC), and Middle Stringer Creek (MSC) and 120 ha for Bubbling Creek (BUB). Creek threshold initiation areas were based on field surveys of channel initiation points in TCEF [*Jencso et al.*, 2009]. Accumulated area entering the stream network was calculated using a triangular multiple flow-direction algorithm [*Seibert and McGlynn*, 2007]. Once the accumulated area exceeded the creek threshold value, it was routed downslope as stream area using a single direction algorithm. To avoid instances where parallel streams were computed, we used the iterative procedure suggested by *McGlynn and Seibert* [2003]. Any stream pixel where we derived more than one adjacent stream pixel in a downslope direction was in the next iteration forced to drain to the downslope stream pixel with the largest accumulated area. We repeated this procedure until a stream network without parallel streams was obtained.

[18] The TCEF riparian areas were mapped based on the field relationship described in the study by *Jencso et al.* [2009]. Landscape analysis-derived riparian area was delineated as all areas less than 2 m in elevation above the stream

network pixel into which they flow. To compare the landscape analysis-derived riparian widths to actual riparian widths at TCEF, *Jencso et al.* [2009] surveyed 90 riparian cross sections in Stringer Creek, Spring Park Creek, and Tenderfoot Creek. A regression relationship (r^2 = 0.97) corroborated their terrain-based riparian extent mapping [*Jencso et al.*, 2009].

[19] The local area entering the stream network is the incremental increase in catchment area for each stream pixel (not counting upstream contributions) and is a combination of hillslope and riparian area on either side of the stream network. We separated local hillslope UAA and riparian area into contributions from each side of the stream following methods developed by *Grabs et al.* [2010]. The UAA measurements for each transect's hillslope were calculated at the toe-slope well position. The riparian buffer ratio was computed as the ratio of local riparian area divided by the local inflows of hillslope area associated with each stream pixel (separately for each side of the stream). The "buffer ratio" represents the capacity of each riparian zone to modulate its adjacent hillslope water inputs. Riparian buffer ratio values were measured at the riparian well position.

[20] *Jencso et al.* [2009] determined the HRS connectivity for the catchments stream network based on a relationship between UAA size and HRS connectivity duration across 24 transects of HRS groundwater recording wells:

$$\%\,\text{Time Connected} = (0.00002 * \text{UAA} - 0.0216) * 100. \quad (1)$$

They found that the duration of a shallow groundwater table connection from hillslopes to the riparian and stream zones was linearly related (r^2 = 0.92) to UAA size. For the purposes of this study, we refer to UAA size as a surrogate for the duration of groundwater table connectivity between HRS zones, based on the relationship observed by *Jencso et al.* [2009]. Larger UAA sizes indicate longer periods of connectivity duration while smaller UAA sizes are indicative of transient connections that only occur during the largest snowmelt events. We applied this relationship to the hillslope UAA values along each stream network in the seven TCEF subcatchments to determine the connectivity to riparian zones through time.

3.2. Hydrometric Monitoring

[21] *Jencso et al.* [2009] instrumented 24 sites in TCEF with transects of shallow recording groundwater wells and piezometers (146 total). At a minimum, groundwater wells were installed across each transect's hillslope (1–5 m above the break in slope), toe slope (the break in slope between riparian and hillslope positions), and riparian position (1–2 m from the stream). All wells were completed to bedrock, and they were screened from 10 cm below the ground surface to their completion depths. Groundwater levels in each well were recorded with Tru Track Inc. capacitance rods (±1 mm resolution) at hourly intervals for the 2007 water year. Hydrologic connectivity between HRS zones was inferred from the presence of saturation measured in well transects spanning the hillslope, toe slope, and riparian positions. Following *Jencso et al.* [2009], we define a hillslope-riparian-stream connection as a time interval during which stream flow occurred, and the riparian, toe slope, and adjacent hillslope wells recorded water levels above bedrock.

[22] Runoff was recorded in each of the seven nested catchments using a combination of Parshall and H-Flumes installed by the USFS (Figure 1). Stage in each flume was measured at hourly intervals with Tru Track Inc. water level recorders and every 15 min by USFS float potentiometers. Manual measurements of both the well groundwater levels (electric tape) and flume stage (visual stage readings) were conducted biweekly during the summer months and monthly during the winter to corroborate capacitance rod measurements.

3.3. Chemical Monitoring

[23] We collected snowmelt, shallow groundwater, and stream samples once a month during the winter, every 1–3 days during snowmelt according to runoff magnitude, and biweekly during the subsequent recession period of the hydrograph. In this paper we highlight the hydrochemical response of four well transects sampled from the 24 transects where physical hydrology was measured. These transects were selected to cover a range of hillslope and riparian area size and the ratio of their areas (riparian buffer ratios). High-frequency solute and SC monitoring was limited to four transects due to the time constraints associated with foot travel across the TCEF catchment during isothermal conditions in a 2 m snowpack. The four transects in this study are named in order of increasing riparian buffer ratios sequentially from one through four (T1–4). Wells were purged to ensure a composite sample along the screened interval before sample collection. Samples for solute analysis were collected in 250 mL high-density polyethylene bottles and filtered through a 0.45 μm polytetrafluorethylene membrane filter. They were stored at 4°C before analyses of major cations with a Metrohm-Peak (Herisau, Switzerland) compact ion chromatograph at Montana State University. Sodium (Na), ammonium (NH_4), potassium (K), calcium (Ca), and magnesium (Mg) were measured on a Metrosep C-2-250 cation column. Detection limits for major cations were 5–10 $\mu g\ L^{-1}$ and accuracy was within 5% of standards. Groundwater specific conductance (SC) was measured with a handheld YSI EC300 meter (±0.1 $\mu S\ cm^{-1}$ resolution and accuracy within ±1% of reading). We also monitored groundwater chemistry and SC in each of the 24 transects installed by *Jencso et al.* [2009] at a bimonthly interval. This corroborated the range of SC dynamics observed at the four transects used in this study and helped to determine base flow SC across the range of riparian zone sizes in TCEF. Stream specific conductance and temperature in each subcatchment's flume was also measured at hourly intervals with Campbell Scientific CS547A conductivity probes (±0.1 $\mu S\ cm^{-1}$ resolution and accuracy within ±1% of reading).

3.4. Specific Conductance as a Tracer of Water Sources

[24] Hillslope shallow groundwater specific conductance was ~80% less than the SC observed in riparian wells during base flow periods of the hydrograph. We used specific conductance to distinguish between hillslope and riparian shallow groundwater and riparian saturation overland flow. Previous studies have used SC to distinguish the spatial sources of water within catchments [*Kobayashi*, 1986; *McDonnell et al.*, 1991; *Hasnain and Thayyen*, 1994; *Caissie et al.*, 1996; *Laudon and Slaymaker*, 1997; *Kobayashi et al.*, 1999; *Ahmad and Hasnain*, 2002; *Covino and McGlynn*,

Table 1. Transect Attributes

Transect	Riparian Soil Depths (m)	Riparian UAA (m^2)	Hillslope UAA (m2)	HRS Connection (days)	Riparian Buffer Ratio	Turnover Time Constant (days)	$t50\%$ Turnover (days)	$t95\%$ Turnover (days)	Riparian Volumes Turned Over
T1	0.7–1.80	783	46112	123	0.017	4	3	13	27
T2	0.7–1.20	163	7070	46	0.023	8	6	25	6
T3	0.6–1.10	1148	10165	29	0.113	29	20	86	1.0
T4	0.7–0.85	700	1527	9	0.458	39	27	115	0.2

2007; *Stewart et al.*, 2007], but validation of SC with its constituent solutes is recommended [*Laudon and Slaymaker*, 1997; *Covino and McGlynn*, 2007]. We compared SC measurements with a composite (n = 126) of major cation concentrations in hillslope, riparian, stream, and snowmelt grab samples determined through IC analysis. A strong linear relationship existed between SC and Ca (r^2 = 0.92) and SC and Mg (r^2 = 0.89) for each spatial source supporting the use of SC as a surrogate tracer for calcium and magnesium concentrations in solution. Hydrochemical tracers, such as Ca^{+}, Mg^{2} are commonly used in comparable studies and when related to Specific conductance, recording SC probes provide high-resolution measurements for source water separations. We restrict the use of SC and solutes as tracers to the snowmelt portion of the hydrograph (1 May 2007 to 1 July 2007) to minimize the potential impacts of weathering and nonconservative behavior.

3.5. Modeling Riparian Groundwater Turnover

[25] We applied a simple continuously stirred tank reactor (CSTR) [*Ramaswami et al.*, 2005]) mixing model to each riparian SC time series to quantify the turnover rate of riparian groundwater in response to hillslope water table development and HRS connectivity. This basic exponential model has been previously used to estimate [*Boyer et al.*, 1997] and model [*Scanlon et al.*, 2001] flushing time constants of dissolved organic carbon and silica from riparian areas and whole catchments.

[26] We fit an exponential decay regression relationship to the riparian well water SC time series at each transect. The time period analyzed for each riparian SC time series was the highest observed SC before snowmelt initiation and HRS connectivity until the time of lowest SC observations. Similar to *Boyer et al.* [1997], we selected sequential data points over this period to determine the linear fit to the relationship between ln(SC) and time. The slopes of these regressions are the turnover rate constants (λ) or how fast the solutes that comprise SC in the riparian reservoir are turned over or mixed with more dilute hillslope inputs. The inverse of this slope represents the "turnover constant" of each site (τ), the time in days it took for the SC in the riparian zone to decrease to 37% of its initial value (Table 1) and for one volume to be flushed [*Ramaswami et al.*, 2005]:

$$\tau = \frac{1}{\lambda}. \tag{2}$$

We believe a more intuitive way of describing exponential decay is the time required for the decaying mixture to decline to 50% of its initial concentration. This is commonly called the half-life and in the context of this paper is referred to as the turnover half-life (t_{50}):

$$t_{50} = \frac{\ln 0.5}{\lambda} = -\tau \ln(0.5) \tag{3}$$

Similarly, we calculated the time it would take to fully turn over all of the original riparian SC in each transect (t_{95}). While an exponential model can never fully reach a baseline concentration, we chose 95% as an acceptable limit at which the riparian zone water SC is deemed similar to water coming from the adjacent hillslope. Thus, 5% of the original riparian SC was considered the baseline at which all initial riparian water was considered turned over from a riparian zone:

$$t_{95} = -\tau \ln(0.05). \tag{4}$$

We also estimated how many riparian volumes moved through the riparian zone at each transect during its corresponding time of HRS connectivity. Riparian volume turnover was calculated by dividing the HRS water table connection duration by the calculated turnover constant:

$$\text{Riparian volumes} = \frac{\text{HRS water table connection duration}}{\tau}. \tag{5}$$

Here we incorporate the duration of the HRS connection; the magnitude of hillslope throughflow associated with each HRS connection is incorporated within the exponential relationship developed from the decay rate of the riparian SC time series.

3.6. Hydrograph Separations for Hillslope, Riparian, and Saturated Area Overland Flow

[27] Hydrograph separations are commonly used tools for separating the spatial and temporal sources of water exiting a catchment. They can provide an integrated measure of source area contributions and their overall effect on hydrologic dynamics observed at the catchment outlet. We implemented 3 component hydrograph separations to determine the spatial contributions to stream runoff from hillslope, riparian, and saturated overland flow sources during the annual snowmelt hydrograph (1 May 2007 to 1 July 07). "Real-time" separations were developed for each subcatchment in TCEF using continuous measurements of riparian-saturated overland flow [*Dewalle et al.*, 1988] and specific conductance.

[28] Saturation overland flow is limited to the near stream riparian areas in TCEF due to upland soils with high infiltration rates. We determined the runoff contributions from riparian overland flow using continuous measurements of

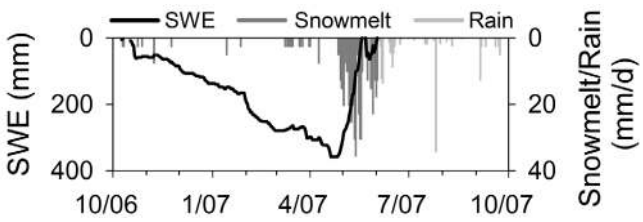

Figure 2. Water year 2007 cumulative snow water equivalent, snowmelt, and rain.

snowmelt rates and riparian area extents delineated with terrain analysis, similar to methods outlined by *Dewalle et al.* [1988]. Riparian snowmelt inputs were computed using a 6 hour exponential smoothing of spatially averaged snowmelt rates obtained from snowmelt lysimeters installed at ST2 and LTC (5 min intervals; Figure 1) and the Onion Park and LSF SNOTEL locations (3 h intervals; Figure 1). Riparian area derived from terrain analysis for each catchment was considered the maximum extent of riparian saturated overland flow. Riparian area saturated overland flow contributions (Q_{RS}) were then calculated as the product of riparian area and average snowmelt rates:

$$Q_{RS} = \text{Catchment riparian area} \times \text{Riparian snowmelt}. \quad (6)$$

Observed stream flow (Q_{ST}) and SC (SC_{ST}) at each subcatchment outlet were adjusted for contributions by saturated riparian overland flow:

$$Q_{STA} = Q_{ST} - Q_{RS} \quad (7)$$

$$SC_{STA} = \frac{(SC_{ST} \times Q_{ST}) - (Q_{RS} \times SC_{RS})}{Q_{ST} - Q_{RS}}, \quad (8)$$

where Q and SC are runoff and specific conductance and the subscripts STA, ST, and RS represent adjusted stream flow, observed stream flow, and riparian overland flow, respectively. Average riparian overland flow SC was held constant at 15 μS cm^{-1} based on average SC measurements of overland flow during snowmelt (n = 70; $\sigma \pm 3$ μS cm^{-1}).

[29] Hillslope and riparian contributions (Q_H and Q_R, respectively) were determined using a traditional two-component hydrograph separation and adjusted stream runoff and SC values:

$$Q_H = \left[\frac{SC_{STA} - SC_R}{SC_H - SC_R}\right] Q_{STA} \quad (9)$$

$$Q_R = \left[\frac{SC_{STA} - SC_H}{SC_R - SC_H}\right] Q_{STA}, \quad (10)$$

where Q and SC are runoff and specific conductance and the subscripts H, R, and STA represent hillslope groundwater, riparian groundwater, and stream flow adjusted for riparian overland flow contributions. Riparian and hillslope groundwater measurements collected from all 24 transects were used to determine their respective end-member SC signatures. We selected three sample time periods (1 October 2006, 18 February 2007, and 26 April 2007) during base flow to determine average riparian groundwater SC. Riparian SC measurements collected during base flow (n = 72) ranged from 92 to 194 μS cm^{-1}. The mean of these was 126 μS cm^{-1}, and the standard deviation was $\pm$36 μS cm^{-1}. Hillslope groundwater SC (n = 88) over the course of the study period was relatively constant ranging from 22 to 39 μS cm^{-1}. The average SC was 27 μS cm^{-1}, and the standard deviation was $\pm$6 μS cm^{-1}. Each spatial source's average SC was used as its end-member SC. Stream flow (Q_{ST}) at the outlet of the TCEF subcatchments was then a mixture of hillslope, riparian, and riparian saturation overland flow (Q_{RS}) components:

$$Q_{ST} = Q_R + Q_H + Q_{RS} \quad (11)$$

and source water contributions were separated continuously during the study period.

[30] We applied uncertainty analyses to the hillslope and riparian separations following the methods of *Genereux* [1998] using

$$W_{fH} = \left\{ \left[\frac{SC_R - SC_{ST}}{(SC_R - SC_H)^2} W sc_H\right]^2 + \left[\frac{SC_{ST} - SC_H}{(SC_R - SC_H)^2} W sc_R\right]^2 + \left[\frac{-1}{(SC_R - SC_H)} W sc_{ST}\right]^2 \right\}^{1/2} \quad (12)$$

$$W_{fR} = \left\{ \left[\frac{SC_H - SC_{ST}}{(SC_H - SC_R)^2} W sc_R\right]^2 + \left[\frac{SC_{ST} - SC_H}{(SC_H - SC_R)^2} W sc_H\right]^2 + \left[\frac{-1}{(SC_H - SC_R)} W sc_{ST}\right]^2 \right\}^{1/2}, \quad (13)$$

where W_{fH} is the relative uncertainty in the hillslope groundwater component, W_{fR} is the relative uncertainty in the riparian groundwater component, Wsc_{ST} is the analytical error in the stream SC measurements, Wsc_H and Wsc_R is the spatial variability of SC in hillslope and riparian groundwater samples (standard deviations of SC for each component), and SC_H, SC_R, and SC_{ST} are hillslope, riparian, and stream SC.

4. Results

4.1. Precipitation Dynamics

[31] We present snow accumulation and melt data from the Upper Tenderfoot Creek (relatively flat 0° aspect, elevation 2259 m) SNOTEL site and rain data from the Stringer Creek tipping bucket rain gauge as a reference for HRS groundwater and runoff response timing in response to precipitation dynamics (Figure 2). The maximum snow pack snow water equivalent before melt was 358 mm. Springtime warming lead to an isothermal snowpack, and most of the snowpack melted between 27 April 2007 to 19 May 2007. Average daily snow water equivalent losses were 15 mm and reached a maximum of 35 mm on 13 May 2007. A final spring snowfall and subsequent melt occurred between 24 May 2007 and 1 June 2007, yielding 97 mm of water.

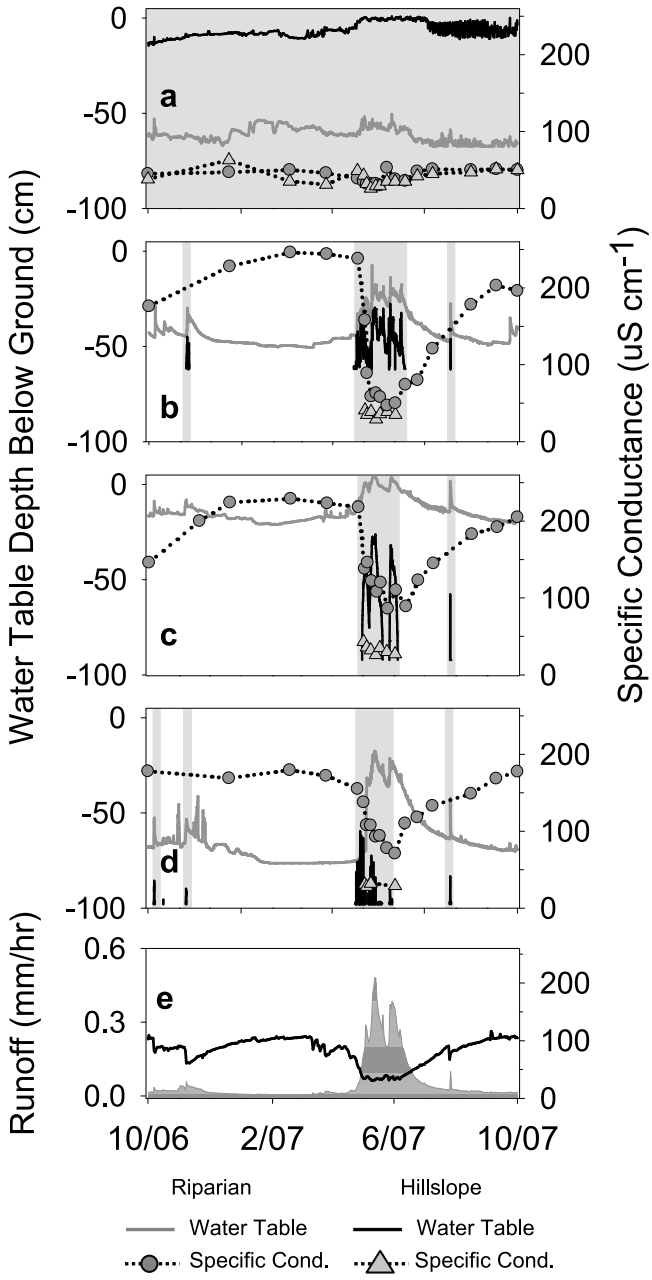

Figure 3. (a–d) Time series of riparian and hillslope water table dynamics and specific conductance at transects 1–4. Times of hillslope-riparian-stream hydrologic connectivity are indicated with gray shading. Runoff (dark gray shading) and specific conductance (black line) dynamics at the Lower Tenderfoot Creek flume are shown (e) for comparison to the transect dynamics.

Four days following the end of snowmelt, two low-intensity rain storms (totaling 30 and 22 mm, respectively) occurred.

4.2. Hillslope and Riparian Hydrologic Connectivity and Specific Conductance Dynamics

[32] We present a detailed description of each transect's landscape attributes and resulting HRS connectivity and SC dynamics in Appendix A. Figure 3 depicts each transects HRS water table connectivity, specific conductance dynamics, and runoff and SC observed at the LTC catchment outlet. Hillslope to riparian water table connectivity ranged from 9 to 123 days across the four transects during the study observation period (1 April 2007 to 1 August 2007; Table 1). Hillslope groundwater was characterized by low specific conductance (~27 μS cm^{-1}, ±6.5 μS cm^{-1}, n = 88). At transects with transient hillslope water tables, riparian groundwater SC was higher during base flow conditions (~127 ± 36 μS cm^{-1}, n = 72) but shifted by varying degrees toward hillslope signatures following HRS connectivity during snowmelt (Figure 3).

4.3. Quantifying the Capacity of the Riparian Zone to "Buffer" Hillslope Connections

[33] When hillslope water tables were present, their SC was consistent and dilute relative to riparian groundwater (Figure 3). Riparian groundwater before spring melt provided a background SC and its change through snowmelt provided an indication of hillslope/riparian mixing, rates of riparian water turnover, and riparian buffering. We applied a CSTR mixing model to each riparian SC time series to quantify the rate of decreasing riparian SC in response to hillslope water table development and HRS connectivity.

[34] During snowmelt, HRS water table connectivity developed across each transect that indirectly led to a significant decrease in riparian SC as more dilute hillslope water entered and mixed with resident riparian water. Each transect exhibited a different turnover rate of riparian water (Figure 4) and goodness of fit to the relationship between ln (SC) and time (r^2 ranging from 0.62 to 0.96). T4, the transect

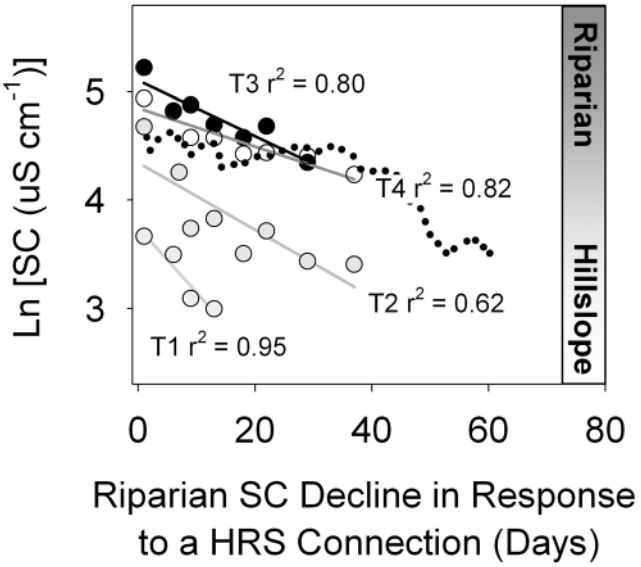

Figure 4. Exponential decline of riparian groundwater specific conductance toward the hillslope signature following the snowmelt induced HRS hydrologic connection. The slopes of these lines indicate the rate of riparian water turnover or dilution by hillslope water. The inverse of the slope is the turnover time constant for each site (Table 1) and provides a measure of riparian buffering of hillslope throughflow. The dotted line represents the exponential decline of LTC stream specific conductance during the same time period.

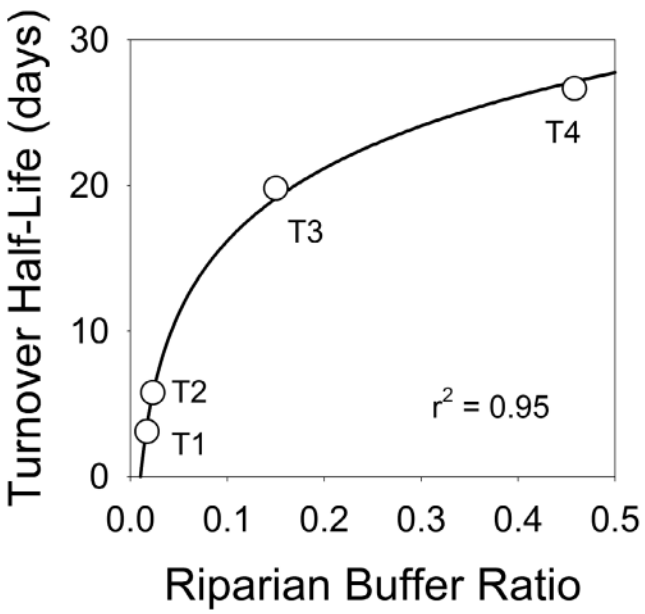

Figure 5. Logarithmic relationship between the riparian buffering ratio (riparian area divided by hillslope area) at each transect and the time that it takes for 50% of the initial riparian concentration to be turned over or diluted by hillslope water (Table 1; equation (2)).

with the lowest frequency of HRS connectivity and a large riparian zone turned over at the slowest rate. In contrast, T1 had a continuous connection throughout snowmelt and the fastest riparian turnover rate. The two intermediary transects (T2 and T3) exhibited sustained HRS connectivity. T2s riparian SC decreased more rapidly from the time of its initial HRS connection relative to T3. T3 had a much larger riparian zone (1148 m^2) compared to T2 (163 m^2), and its riparian zone was connected to the hillslope for a shorter duration (Table 1).

[35] We plotted the time it took for each riparian zone's SC to decrease to half of its initial value (t_{50}, equation (3)) against its riparian buffer ratio (riparian area/hillslope area) to determine the potential of each riparian zone to modulate its corresponding hillslope water table connection. We found a logarithmic relationship between the buffer ratio and the t_{50} time (r^2 = 0.95) at each transect (Figure 5; equation (14)):

$$t_{50} = 6.13 \ln(\text{Riparian buffer ratio}) + 29. \quad (14)$$

T1 had the lowest buffer ratio, and it took only 3 days for the riparian SC to be reduced by half by hillslope inputs. During its continuous HRS connectivity throughout the study period (123 days), approximately 27 riparian volumes were turned over (equation (5); Table 1). T2 had a small riparian area relative to its hillslope connection duration and the second shortest turnover half-life (6 days). Six riparian volumes were exchanged in T2 during its 46 day HRS connectivity time period. The turnover half-life for T3 was 20 days, and ~1 riparian volume of mixed hillslope and riparian water was removed during its 29 day HRS connectivity time period. T4 had the longest observed turnover half-life (27 days) associated with its large riparian buffering ratio. Only 26% of the original riparian volume was turned over during its 9 day HRS connectivity duration.

[36] One or more (up to 27) riparian volumes passed through the transects (T1 and T2) with low riparian buffering ratios and sustained HRS connections resulting in a predominantly hillslope water SC signature in these riparian zones. The two transects (T3 and T4) with larger buffer ratios never approached hillslope SC during their HRS connectivity duration. We calculated the time it would take to deplete the original riparian SC at each transect (equation (4)) to evaluate the effect of changing HRS connectivity duration on the degree of turnover that can occur at each transect.

[37] Figure 6 illustrates the time required; incorporating each transect's time constant, for the initial riparian water to be mixed or replaced by dilute hillslope inflows. T4 would require 115 days to completely turn over its riparian water, but it was only connected for a total of 9 days during snowmelt. T3 would require 86 days to turn over but was only connected 29 days. T2 would require 25 days, which was less than its observed 46 day HRS connection duration. This was consistent with the observed riparian SC time series (Figure 3b) that indicated that riparian SC decreased to the hillslope groundwater SC over the course of spring runoff. Similarly, T1's riparian zone only required 13 days to fully turn over, and its SC dynamics followed those of the hillslope throughout its continuous connectivity duration.

4.4. Comparing Internal Distributions of Riparian Buffering and Turnover to Source Water Separations at the Catchment Outlet

[38] Plot scale hydrochemical time series indicated that the size of a riparian zone relative to duration of groundwater connectivity to its uplands (as represented by UAA size [*Jencso et al.*, 2009]) may be a predictor of the turnover rate of riparian water (equation (14); Figure 5). Riparian and

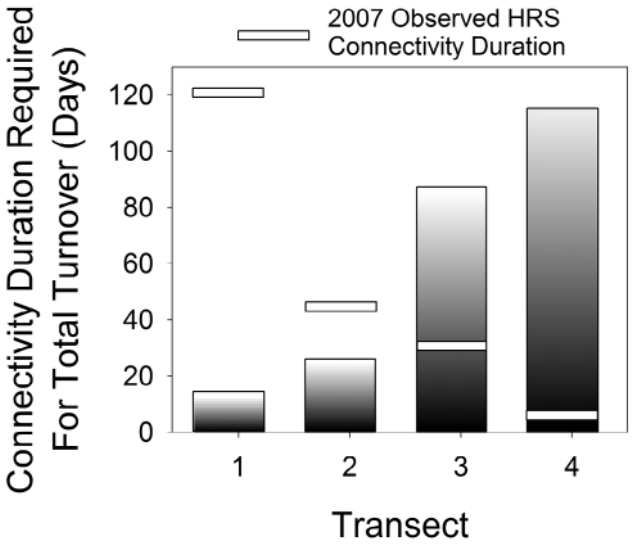

Figure 6. Estimated hillslope-riparian-stream connectivity duration required for 95% of the initial riparian water to be replaced or diluted by hillslope throughflow (shaded bars) and the observed HRS connectivity duration for the study observation period (white rectangles). The riparian zone is estimated to be turned over when SC reaches hillslope signatures (white shading) denoted in each shaded bar.

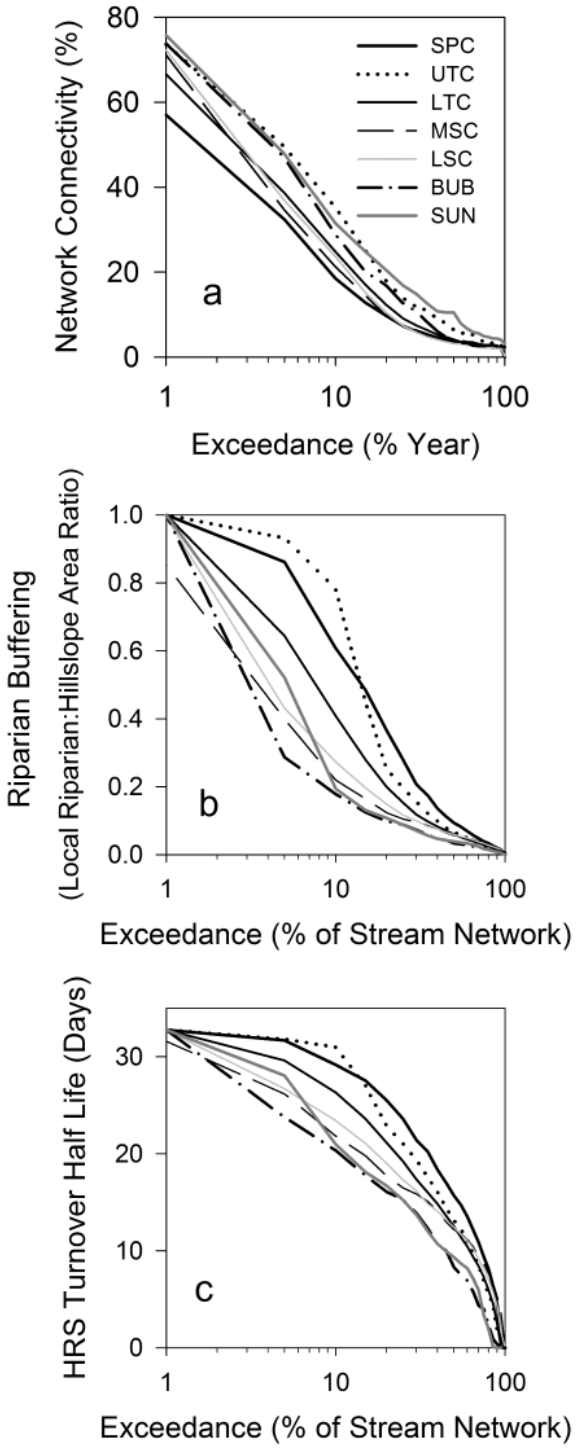

Figure 7. TCEF subcatchment distributions of stream network (a) HRS connectivity, (b) riparian buffering, and the resultant (c) riparian groundwater turnover times. Riparian water turnover times (riparian buffering) are a function of hydrologic connectivity and the size of the riparian area relative to the adjacent hillslope. Catchments with fast turnover times had more sustained HRS connectivity and less riparian buffering of hillslope inputs. Catchments with longer duration turnover times had shorter duration hillslope groundwater table connectivity to their riparian zones and more effective riparian buffering along the stream network.

hillslope area typically are not distributed homogenously along stream networks. Different distributions and combinations of each can be found in neighboring catchments according to their landscape structure [*McGlynn and Seibert*, 2003]. We examined how HRS connectivity durations (function of UAA), riparian buffering, and riparian groundwater turnover were distributed within each subcatchment in TCEF (Figure 7).

[39] Figure 7a illustrates connectivity duration curves (CDCs) [*Jencso et al.*, 2009] for each stream network. Each CDC was derived from the combined 10 m left and right stream bank frequencies of HRS connectivity for the 2007 water year (equation (1)). Catchments with less topographic complexity and a higher proportion of larger UAA sizes exhibited elevated annual HRS connectivity and a higher magnitude peak connectivity. Decreased annual connectivity and lower magnitude peak connectivity was characteristic of catchments with more convergence and divergence in the landscape and a higher frequency of small UAA sizes.

[40] How riparian areas were arranged next to their adjacent hillslopes determined the distribution of stream network riparian buffering (Figure 7b) and the resultant turnover times (equation (14); Figure 7c). Catchments with a higher frequency of larger UAA relative to riparian extents had less stream network riparian buffering and a higher frequency of fast riparian groundwater turnover times (and vice versa).

[41] We compared the distribution of riparian buffering and turnover with the timing and total amounts of riparian groundwater in each subcatchment's annual snowmelt hydrograph (Table 2). To elucidate potential differences of source water contributions across catchments, we determined the percentage of riparian, hillslope, and riparian overland flow contributions to the snowmelt hydrograph before snowmelt (1 April), and during the rising (1 May), peak (14 May), and recession (1 July) of the hydrograph. Figure 8 depicts riparian buffering maps, estimated turnover along the stream network, and snowmelt hydrograph separations for SPC, LSC, and SUN catchments. These catchments span the range of turnover distributions and resultant riparian groundwater contributions found across all seven nested catchments within TCEF (Figure 9).

[42] SPC was characteristic of catchments with a high degree of riparian buffering (Figures 7b and 8a) and long duration riparian turnover times (Figures 7c and 8d). A significant amount of riparian area and buffering potential is accumulated along the two headwater tributaries of SPC and its mainstem (Figure 8a). This resulted in a high proportion of long duration turnover times along the stream network (Figure 8d) and a median catchment riparian turnover half-life of 15.3 days (Table 2 and Figure 7c). SPC also had the largest riparian groundwater contribution in its annual snowmelt hydrograph (Table 2 and Figure 9, SPC). Total riparian runoff was 97.4 mm for the entire study period. Riparian groundwater contributions were persistent before snowmelt (61%) and during the rising (26%), peak (30%), and falling limb (53%) of the annual snowmelt hydrograph (Figure 8g).

[43] LSC was more characteristic of other TCEF catchments (UTC, LTC, and MSF) with more moderate values of riparian buffering (Figure 8b) and turnover half-life values along their stream length (Figure 7c UTC, LTC, MSC, and LSC, and Figure 8e). Within these catchments, the majority

Table 2. Tenderfoot Creek Experimental Forest Catchment Landscape Distributions and Riparian Turnover and Runoff

Catchment	% Riparian Area	Median Hillslope UAA (m^2)	Median Riparian UAA (m^2)	Median Buffer Ratio	Median $t50$ time (days)	Total Riparian Runoff (mm)	Riparian Runoff (%)
SPC	6.10	1695	148	0.1330	15.3	97.4	36
UTC	4.99	3510	167	0.0640	12.98	34.8	17
LSC	3.0	2357	148	0.0591	12.5	45.0	14
LTC	3.90	2403	145	0.0597	12.6	39.7	12
MSC	3.10	2983	181	0.0578	12.45	37.9	11.3
SUN	1.70	4488	156	0.0419	9.8	4.8	1.9
BUB	0.89	3345	124	0.0348	9.3	3.2	1.3

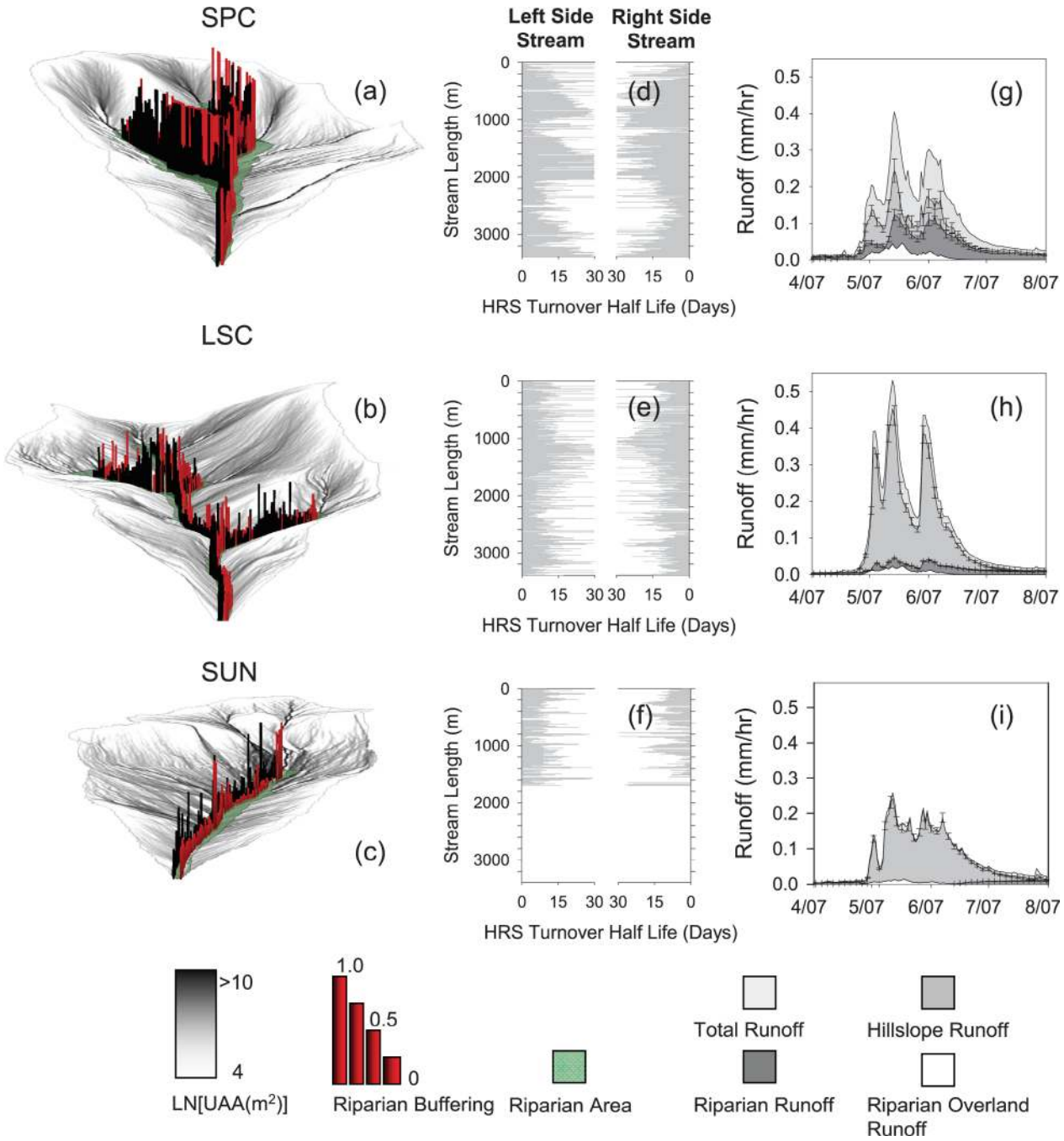

Figure 8. Subcatchment (a–c) hillslope UAA, riparian area, and riparian buffering potential (black and red bars), (d–f) the HRS stream network turnover distribution derived from the riparian buffering-turnover relationship (equation (5)), and (g–i) spatial source water separations for each subcatchment. Catchments with higher riparian buffering and turnover time distributions have a more sustained riparian groundwater contribution to their annual snowmelt hydrographs.

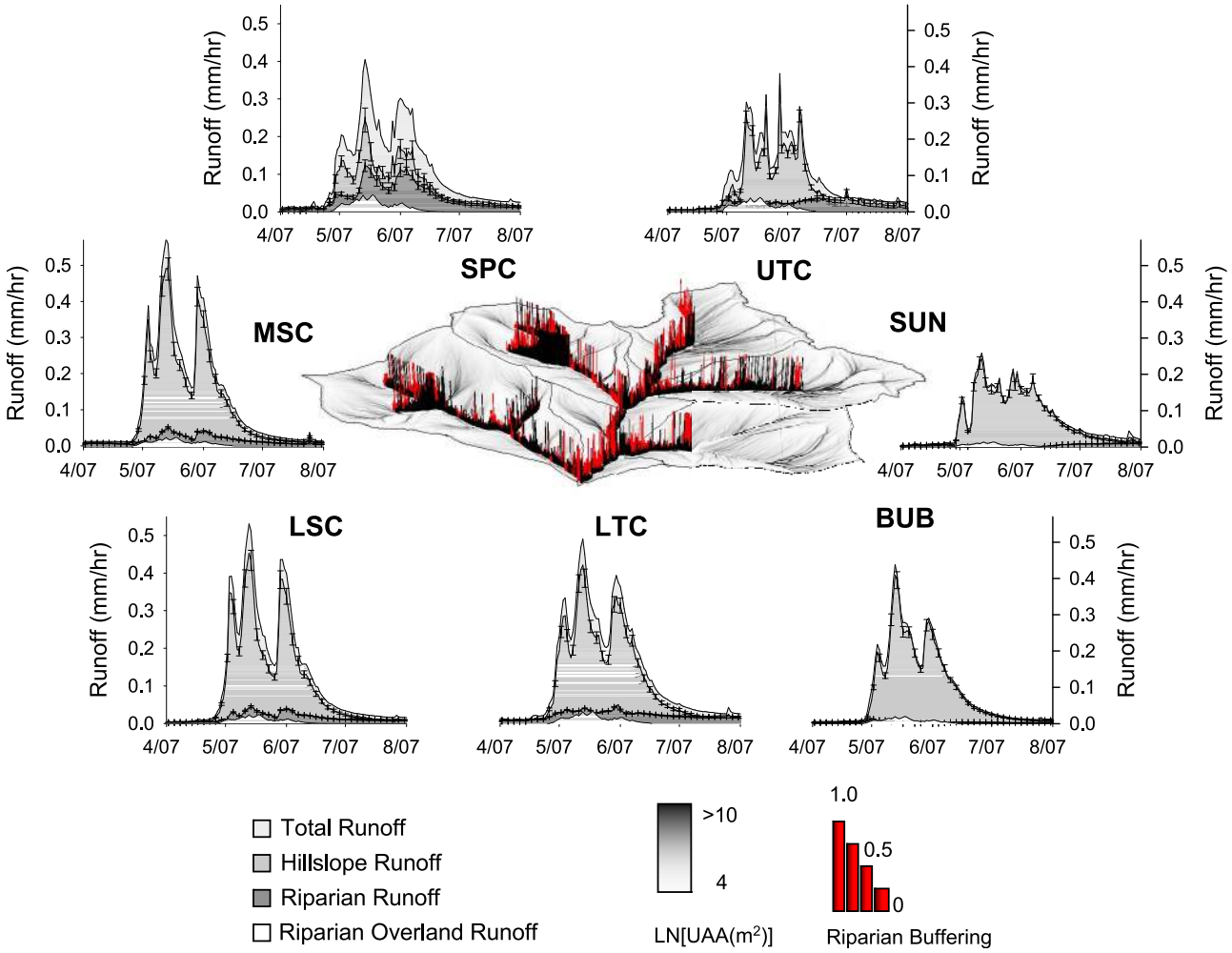

Figure 9. Spatial source water separations for the TCEF subcatchments and the TCEF UAA accumulation patterns and stream network riparian buffering (ratio of local riparian and hillslope area). Runoff was separated into hillslope, riparian, and riparian saturation overland flow components. Error bars indicate the uncertainty in the hillslope and riparian components. The frequency of different magnitude riparian buffering and turnover times along the stream network determined the spatial sources of water detected at each catchment's outlet. Catchments with a greater frequency of high riparian buffering of hillslope inputs and long turnover times had more sustained riparian contributions in their snowmelt hydrographs.

of large riparian buffering values are positioned along the catchment headwaters and at interdispersed locations along each stream network's main stem (Figure 8b). The extent of riparian area relative to hillslope area inputs at the majority of stream network positions is smaller and hillslope inputs were often more focused through small riparian zones. This resulted in less riparian buffering along the stream network (median buffer ratio 0.64–0.59; Table 2) relative to SPC and median catchment riparian turnover half-lives ranging from 12.5 to 13.0 days. Riparian and hillslope groundwater contributions were also more typical of TCEF catchments with moderate t_{50} distributions (UTC, LTC, MSC, and LSC: Figure 8h; Figure 9). As an example, LSC's percent riparian runoff contributions decreased during the transition from base flow (58%) to the rising limb (17%). The magnitude of riparian runoff increased throughout the peak of the snowmelt hydrograph and was synchronous with runoff dynamics, albeit it was a small percentage of total runoff (12%) relative to hillslope contributions. During the recession, riparian runoff increased to 32%. Total riparian runoff for LSC during the snowmelt period was 45 mm, within the range (34.8–45.0 mm) observed for other TCEF catchments with moderate t_{50} times.

[44] SUN and BUB creek were characteristic of catchments with the highest frequency of small riparian buffering values (Figures 7c and 8c) and t_{50} times (Figure 7c SUN and BUB, and Figure 8f) along the stream network. Both are first-order stream networks with less dissected hillslope topography and higher median hillslope inflows (Table 2) that are more evenly distributed along the stream network (Figure 8c). They also have the smallest percentages of total riparian area (1.70 and 0.89) along their stream networks and minimal buffering of hillslope UAA (Figure 8c). The combination of small riparian area relative to large hillslope UAA sizes resulted in a high frequency of fast riparian turnover times (Figure 8f) and median catchment turnover half-lives of 9.8 and 9.3 days (Figure 7c SUN and BUB). Riparian groundwater contributions were also typical of TCEF catchments with fast riparian turnover times (Table 2 and Figure 9 SUN and BUB). For example, SUN's base

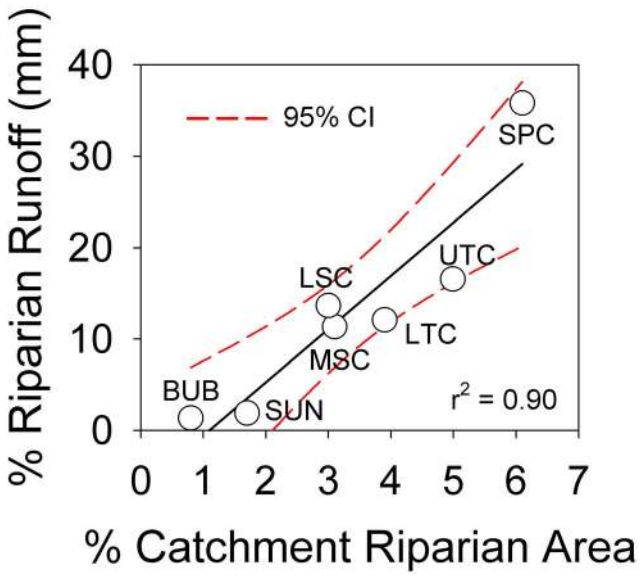

Figure 10. The riparian percentage of total runoff during the snowmelt period plotted against the percentage of riparian area for each TCEF catchment.

flow riparian contributions initially comprised 67% of runoff. Riparian contributions initially increased during the rising limb but decreased to only 1% during peak runoff (Figure 8i; Figure 9 SUN and BUB). During the recession, riparian contributions progressively increased to 17% of total runoff. Total riparian runoff for SUN was small (4.8 mm) relative to the majority of the other TCEF catchments. BUB was the other TCEF catchment with a similar median turnover time (9.3 days), and it exhibited similar riparian runoff dynamics (Figure 9 BUB and Table 2) and total contributions (3.8 mm).

[45] We compared the percentage of each catchment's total riparian area to its total riparian runoff contributions during the snowmelt hydrograph (Figure 10). A strong linear relationship (r^2 = 0.90) suggested that increasing total catchment riparian area can result in increased riparian groundwater contributions. While this relationship was strong, it provides little insight into the relationship between the internal interactions and connections that can occur between hillslope and riparian settings within a catchment.

[46] We also plotted the median value of each catchments t_{50} time (equation (2); Figure 7) against its riparian groundwater contribution (Figure 9) to better elucidate how the distribution of water table connectivity (as represented by hillslope UAA size [*Jencso et al.*, 2009]) among local hillslope and riparian area assemblages can affect whole watershed response (Figure 11). The amount of riparian runoff exiting each catchment increased linearly with increasing catchment median t_{50} time duration (Figure 11; r^2 = 0.91).

5. Discussion

5.1. What is the Effect of HRS Connectivity Duration on the Degree of Turnover of Water and Solutes in Riparian Zones?

[47] Transient hillslope groundwater tables are important to the timing and magnitude of runoff and delivery of solutes to stream networks. Equally important is the potential for the riparian zone to buffer hillslope groundwater inputs and thereby stream water composition. We investigated shallow groundwater hydrologic and specific conductance (as a surrogate of solute concentrations) dynamics across four hillslope-riparian-stream (HRS) transects with different riparian and hillslope sizes to ascertain controls on riparian buffering of hillslope runoff and the resulting expression of hillslope solute signatures in stream water. Our results indicate that the intersection of HRS connectivity (as controlled by hillslope UAA size [*Jencso et al.*, 2009]) with riparian area extents is a first-order control on the degree of riparian water turnover during snowmelt.

[48] Stream positions with riparian zones adjacent to larger hillslope UAA were poorly buffered. These positions had longer duration hillslope-riparian-stream hydrologic connectivity (T1 and T2) and riparian groundwater SC that maintained or approached hillslope SC signatures over the course of spring runoff (Figure 4, T1 and T2). This indicated that riparian water in the riparian zone before snowmelt was fully mixed and displaced by hillslope groundwater with connectivity initiation and maintenance. For example, T1, the HRS sequence with the largest hillslope UAA size and continuous HRS hydrologic connectivity, had the fastest turnover time (3 days) across the four transects under observation. The riparian zone of T1 was relatively large compared to other transects with longer turnover times. However, riparian groundwater SC was always similar to hillslope groundwater SC (Figure 3a). This suggests that the continuous delivery of hillslope water to the riparian zone minimized its buffering potential. Along HRS sequences with large hillslope UAA relative to riparian area extents,

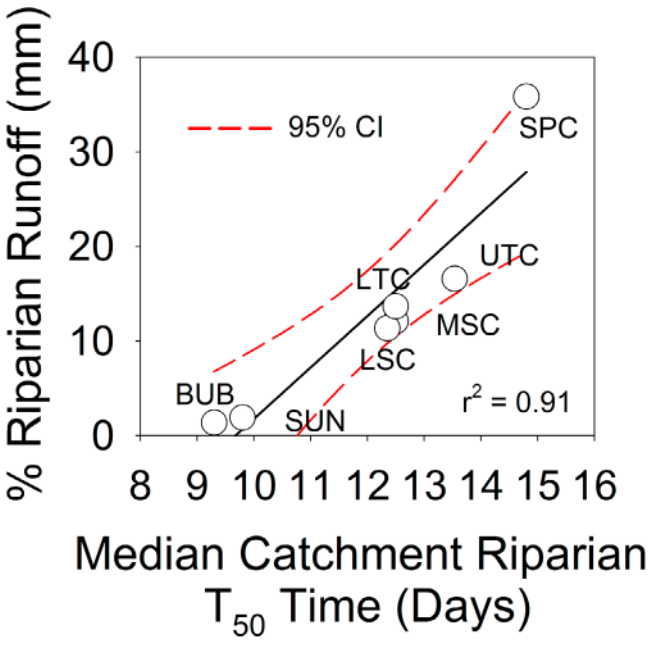

Figure 11. The percentage of riparian runoff during the snowmelt period plotted against the median of the riparian turnover half life distribution for each TCEF subcatchment. The total riparian runoff observed at each catchment outlet was a function of the distribution of riparian turnover times within each catchment.

the riparian zone exerts minimal control on stream water composition.

[49] Stream positions with larger riparian zones adjacent to smaller hillslope inputs were better buffered. These positions (T3 and T4) exhibited shorter duration HRS hydrologic connectivity [*Jencso et al.*, 2009], and riparian groundwater SC never reached hillslope groundwater signatures. The rate of riparian SC decline was also less than along transects with smaller riparian: hillslope zone buffer ratios (Figure 4). This is exemplified in transect T3 where the HRS hydrologic connection was sustained for 29 days during the snowmelt period and the riparian zone was the largest under observation. Only one riparian volume was turned over along T3 during its connectivity duration. Transect 4 exhibited transient hillslope connectivity (9 days) relative to its medium-sized riparian zone. This resulted in the greatest observed riparian buffering and turnover of only 26% of the original riparian water in response to HRS connectivity. These dynamics suggest that the decline of riparian groundwater SC toward hillslope signatures was limited by the HRS hydrologic connectivity duration and the relatively large amount of water stored in the riparian zone before connectivity initiation.

[50] This study has considered the topographically driven connections that can initiate riparian groundwater turnover and mixing during wetter catchment states. While topographic controls were strong across all four transects, each exhibited a different goodness of fit relationship between the dilution in riparian SC and time (Figure 4; r^2 ranging from 0.62 to 0.96). These differences could be associated with additional controls on riparian groundwater turnover including vertical infiltration of snowmelt directly into the riparian zone and/or incomplete mixing of riparian and hillslope groundwater. Emergence of groundwater from deeper bedrock flow paths [*Vidon and Smith*, 2007], stream water ingress to the riparian zone [*Burt et al.*, 2002; *Duval and Hill*, 2006], and down valley shifts in equipotential gradients [*Larkin and Sharp*, 1992; *Vidon and Hill*, 2004b] could also introduce complexities in stream reaches with different morphologies and during drier time periods.

[51] In this investigation, HRS connectivity initiation and duration was the primary driver of riparian water and solute turnover during the snowmelt period. We suggest that the ratio between riparian and hillslope area can be interpreted as a buffer capacity index (Figure 5) within a landscape analysis framework [*McGlynn and Seibert*, 2003] and, when combined with estimates of connectivity duration [*Jencso et al.*, 2009], can provide a surrogate measure of the groundwater turnover/mixing that occurs along individual HRS landscape sequences in a stream network.

[52] Physical hydrologic mechanisms (e.g., hydrologic connectivity and riparian water turnover dynamics) are important context, and we suggest necessary considerations before one interprets and attempts to quantify biogeochemical cycling and water quality buffering potential in riparian zones [*Peterjohn and Correll*, 1984]. For example, a common finding across field studies of riparian zones in diverse landscape settings is the importance of water movement rates on the potential for nitrate removal from shallow groundwater via denitrification [*Burt and Arkell*, 1987; *Lowrance*, 1992; *Hill*, 1996; *Creed and Band*, 1998; *Welsch et al.*, 2001; *Vidon and Hill*, 2004b]. Water quality functions often attributed to riparian areas can be strongly affected by the rate of water movement [*Schlesinger*, 1991] and together with biogeochemical transformations and simple volume buffering can mediate streamwater nutrient loading.

[53] Variability in the duration of connectivity between hillslopes and riparian zones is also important to consider when assessing riparian buffering efficacy through time. Landscape-scale results suggested turnover dynamics will be variable from year to year in response to changes in precipitation magnitude, duration, and frequency. For example, in this study, T4 would have required 115 days (31% of the water year) of HRS connectivity to fully turn over the adjacent riparian zone (Table 1 and Figure 6). However, the hillslope UAA for this transect was 1527 m^2, and typical HRS groundwater connectivity dynamics reported for hillslopes in this UAA size range by *Jencso et al.* [2009] were limited to ~29 days (8% of the water year). A substantial increase in annual precipitation would be required to sustain HRS connectivity duration at T4 to 115 days and fully turn over riparian zone water. This suggests that some riparian positions along the stream network could shift from well to poorly buffered in wetter years. Alternatively, a decrease in annual precipitation would decrease the HRS connectivity duration across the entire range of UAA sizes and result in less mixing and displacement of riparian groundwater and subsequently more effective riparian buffering of hillslope runoff. Both of these scenarios suggest significant interplay between climate variability, stream source water contributions, and riparian buffering efficiency across time.

5.2. How Does Landscape Structure Influence Stream Network Hydrologic Dynamics and the Timing and Amount of Source Waters Detected at the Catchment Outlet?

[54] The relationship between landscape structure and runoff generation, timing, and mixing dynamics has been difficult to interpret. Investigations utilizing source water separations at the catchment outlet have suggested that contributions of hillslope and riparian zone water to streamflow are proportional to hillslope and riparian size arrangements and the degree of hydrologic connectivity that occurs between them [*McGlynn and McDonnell*, 2003b]. However, little research to date has investigated landscape-scale hillslope and riparian shallow groundwater connectivity and mixing dynamics and how they are distributed across entire stream networks.

[55] Our results demonstrated that landscape structure strongly influenced the maximum HRS shallow groundwater connectivity (ranging from 56% to 80% of the stream network) and its temporal change within each catchment. Topographic convergence and divergence in the landscape is one measure of catchment complexity and is reflected in the frequency distribution of hillslope upslope accumulated area sizes along the stream network. Catchments (e.g., SPC) with more dissected landscapes had more diffuse hillslope area inputs and lower median catchment UAA values. This resulted in a higher proportion of short duration HRS connectivity along the stream network and less HRS connectivity during peak snowmelt (~56% network connectivity in SPC; Figure 7a). Less dissected catchments (e.g., SUN) had higher median UAA values, elevated annual connectivity, and higher maximum HRS network connectivity (~80% network connectivity in SUN; Figure 7a).

[56] The intersection of hillslope area accumulation with its adjacent riparian area indicated riparian buffering potential (equation (14)). We measured an order of magnitude difference in the median riparian buffering values across the seven subcatchments even though they had similar median riparian extents (Table 2). This was a result of the spatial organization of hillslope area accumulation relative to riparian area extents along the stream network. Catchment topography and topology resulted in some catchments with more diffuse inputs of hillslope area adjacent to large riparian areas and higher median riparian buffering values (Figures 7b and 8a). Lower median riparian buffering occurred in the catchments with less convergence/divergence that focused larger hillslope inputs into smaller riparian zones (Figures 7b and 8c).

[57] Each catchment's riparian buffering (Figure 7b) and riparian turnover (Figure 7c) frequency distributions suggested that large differences in the riparian and hillslope groundwater components would be detected in catchment runoff. Catchments with higher riparian buffering would have less riparian groundwater turnover and less expression of hillslope groundwater in their snowmelt hydrographs. Lower median riparian buffering and faster riparian turnover would lead to greater hillslope contributions to streamflow as riparian zones flush in response to more sustained hillslope connectivity. Independently determined source water hydrograph separations supported these hypotheses derived from landscape analyses (Figure 11). Total riparian runoff from each of the seven catchments ranged from 3 to 97 mm during the seasonal snowmelt period. This is nearly an order of magnitude difference in riparian groundwater contributions between the seven headwater catchments; all of which are within 5 km of one another within the greater 22.8 km^2 Tenderfoot Creek catchment.

[58] Catchment structure also appeared to control the timing of riparian and hillslope groundwater expressed in runoff. When HRS connectivity is initiated, water moves from hillslopes through riparian zones to the stream resulting in increased stream flow. However, the hillslope water first mixes with and displaces groundwater stored in the riparian zones before the event (Figure 4). In general, a larger riparian zone results in longer turnover times of the preconnectivity riparian chemical signature (Figure 5) and a more sustained riparian groundwater contribution to stream flow. Hydrograph separation results from each catchment indicated an increase in riparian contributions with snowmelt (Figure 11), initiated by HRS connectivity (Figure 3) [*Jencso et al.*, 2009] and mixing and displacement of riparian water by hillslope water (Figure 4). However, the persistence of a riparian signature in each hydrograph varied according to the timing of turnover across each stream network (e.g., Figures 8d, 8e, and 8f). This suggests that the frequency of different HRS connectivity durations across the watershed controls runoff magnitude [*Jencso et al.*, 2009], but it is the intersection of connectivity and the turnover dynamics of the adjacent riparian reservoirs that controls the source water signature of the stream (as the mixture of hillslope and riparian source waters) through time.

[59] Our observations suggest that each catchment's structure largely controlled the hydrologic and solute dynamics measured in stream flow. Variability in landscape structure can influence the timing, magnitude, and location of water delivery from uplands to near-stream areas during a storm event. The interaction/intersection of hillslope water and water stored in the riparian zones determines the timing and proportion of source waters measured at the catchment outlets. These observations suggest a degree of predictability when estimating where in the landscape runoff is generated and its source water composition through time in catchments of differing size and structure.

5.3. Landscape Connectivity Conceptual Model of Runoff Generation, Riparian Buffering, and Source Water Mixing

[60] Many field studies have characterized the heterogeneity of hydrologic response at the plot, landscape, and catchment scales. This has resulted in the development of detailed and complex characterizations of catchment dynamics but little transferability of general principles across catchment divides. We suggest hydrologic connectivity as a "mechanism to whittle down unnecessary details and transfer dominant process understanding from the hillslope to the catchment scales [*Sivapalan*, 2003]." The following paragraphs present a simple conceptual model of catchment response to snowmelt and precipitation events based on the relationships between landscape structure, metrics of HRS hydrologic connectivity, and riparian buffering.

[61] *Jencso et al.* [2009] found that the magnitude of runoff generation in one watershed at the TCEF was driven by variability in hillslope UAA size distributions and the frequency of their lateral connections along the stream network. During base flow periods, the majority of the stream network's riparian zones were hydrologically disconnected from their uplands except those adjacent to the largest hillslopes. As snowmelt proceeded HRS connectivity was initiated across progressively smaller hillslope UAA sizes and runoff increased with each subsequent connection. Here we suggest that the sequencing of connectivity initiation (according to topography and topology) across the stream network determines runoff magnitude through time, but that it is the intersection of connectivity frequency and duration with riparian area extents that controls riparian buffering and source water components measured at the catchment outlet.

[62] A spectrum of riparian groundwater turnover times is possible in a given watershed according to the arrangement of hillslope and riparian sizes. HRS sequences with large hillslope UAA (more persistent connections) relative to riparian area will turn over quickly and contribute predominantly hillslope water during the course of an event. At the other end of the spectrum, HRS sequences with small hillslope UAA (transient connections) and larger riparian zones will be well buffered against hillslope throughflow and contribute a more persistent quantity of riparian groundwater to the stream. Therefore, a catchment's buffering efficacy and outlet source water dynamics are a result of an integration of the frequency and timing of HRS hydrologic connectivity and associated riparian buffering (turnover) across the stream network. If the riparian buffering potential exceeds its connectivity duration across the network, then a riparian groundwater contribution will dominate the stream hydrograph. However, greater hillslope connectivity and lower riparian buffering will result in increased turnover of riparian groundwater and a greater hillslope source water signature measured at the catchment outlet. Each watershed

progresses from the well to poorly buffered case through time and with increasing antecedent wetness and event size and duration.

[63] The value of a conceptual hydrologic model can be measured by its ability to be effectively transferred to alternate catchments. Contributions of runoff and solutes to the TCEF stream network are highly variable in time and space and largely driven by the topographic redistribution of water from the uplands, through riparian zones, and into the stream network. Many studies have observed strong relationships between landscape topography and runoff generation [*Dunne and Black*, 1970; *Anderson and Burt*, 1978; *Beven*, 1978; *Burt and Butcher*, 1985], runoff spatial sources [*Sidle et al.*, 2000; *McGlynn and McDonnell*, 2003b], and water residence times [*McGlynn et al.*, 2004; *McGuire et al.*, 2005; *Tetzlaff et al.*, 2009]. This suggests that metrics of topography, topology, and resulting connectivity could be an organizing principle for predicting storm response in headwater catchments. In other environments, bedrock geology [*Huff et al.*, 1982; *Wolock et al.*, 1997; *Burns et al.*, 1998; *Shaman et al.*, 2004; *Uchida et al.*, 2005], soil characteristics [*Buttle et al.*, 2004; *Devito et al.*, 2005; *Soulsby et al.*, 2006; *Tetzlaff et al.*, 2009], or other catchment features could additionally influence and even dominate connectivity between source areas and the stream network.

[64] Variability in patterns of topography, soils, geology, and climate all influence runoff generation. However, their combined effect and relative importance for streamflow dynamics has been difficult to decipher. To attribute appropriate causal mechanisms to catchment outlet response, we emphasize the importance of internal/distributed hydrologic monitoring across time. Changing soil moisture states and the transition from vertical to lateral connectivity in the shallow subsurface [*Grayson et al.*, 1997] or the partitioning of water to/from deeper bedrock storage [*Sidle et al.*, 2000; *Shaman et al.*, 2004; *Uchida et al.*, 2005] can significantly alter water sources observed in streamflow. For example, a recent distributed assessment of the stream network water balance at Tenderfoot Creek indicated that runoff generation transitioned from topographically driven lateral redistribution of water and hydrologic connectivity [*Jencso et al.*, 2009] at wetter catchment states to detectable geologic controls (~10% stream network connectivity) at low base flow [*Payn et al.*, 2009]. This suggests a potential transition in streamflow generation mechanisms as a function of catchment wetness state.

[65] Consideration of hydrologic connections and source areas within the landscape is critical to deconvolution of catchment outlet dynamics into their spatial sources and controlling mobilization processes. We suggest that the conceptualization presented here provides a simple and potentially robust description of runoff response across catchments of different size and structure and may prove useful for prediction in ungauged basins.

5.4. Watershed Management Implications of Riparian Buffering of Landscape Hydrologic Connectivity

[66] Riparian zone management to protect and promote water quality is a valuable strategy across natural and disturbed landscapes. However, few tools exist to aid prioritization of riparian management by assessing the relative importance of riparian zones across the landscape and their potential to influence upland runoff and associated water quality constituents [*Allan et al.*, 2008]. In this paper we have presented a hydrological context and volumetric buffering quantification that considers not only riparian zone size and fraction of the total catchment but also an estimate of each riparian zone's buffering potential relative to the upland delivery of runoff. We focused on the physical hydrology and tracer behavior across riparian zones. However, this context is also critical for understanding potential for biogeochemical transformations because it demonstrates the primary landscape controls on riparian water turnover rates and magnitude and provides tools to quantify these processes. For example, water delivery from hillslopes can influence the supply of oxygenated water to carbon-rich riparian zones thereby influencing redox state and the potential for microbial denitrification [*Hill*, 2000; *Vidon and Hill*, 2004a]. Better assessment of riparian zone potential to mitigate upland water quality degradation, new methods to aide prioritization of riparian management and protection across space, and tools to assess catchment-scale riparian buffering potential or conversely catchment sensitivity to upland loading have strong relevance to watershed management and applied hydrology-biogeochemistry applications. We suggest that research presented here provides some initial insight not only into how we might better characterize and quantify riparian zone buffering potential at the reach and catchment scales but also highlight the need for tools to bring these concepts to the riparian and watershed management communities.

6. Conclusion

[67] Hydrological science continues to search for insights into catchment response based on landscape structure. The research described in this paper highlights terrain metrics that link hydrologic process observations to landscape and catchment scale response. This approach discretizes the catchment into its component landscape elements and analyzes their topographic and topologic attributes as surrogates for their hydrologic connectedness, as measured through detailed field observations. On the basis of our high-frequency monitoring of groundwater connectivity and solute dynamics from the plot to catchment scales we conclude

[68] • The degree of riparian water turnover (riparian buffering) is a function of hydrologic connectivity and the size of the riparian area relative to the adjacent hillslope.

[69] • The frequency of stream network hydrologic connectivity and associated degree of riparian buffering (turnover) control the timing and magnitude of catchment runoff and solute export.

[70] • Catchment structure/organization strongly affects riparian buffering and runoff source water composition.

[71] • Climate variability (wet or dry years) may introduce a "quantifiable" shift in stream network connectivity and the mobilization of water and solutes from riparian and hillslope source areas.

[72] Discretization of catchments into their component landscape elements and monitoring the hydrochemical response in these landscape elements and by comparing catchments of varying structure provided insight into the spatial sources of runoff that are hidden by hydrograph separations measured at the catchment outlet alone. This approach allowed us to estimate where runoff and solute mobilization occurred within the landscape and how the

integration of these dynamics along the stream network relate to the magnitude of runoff and solute export across catchments of differing scale and structure.

Appendix A

[73] We present specific conductance and water table results for each transect in order of increasing riparian buffer ratios (riparian area/hillslope area) and decreasing hillslope UAA size and connectivity duration (Figure 3).

[74] Transect 1 (T1) was located at the base of a ~20.5° convergent hillslope. It had the largest observed UAA (46,112 m^2) of any of the 24 transects, a medium-sized riparian area (783 m^2), and the lowest buffer ratio (0.017). The riparian zone exhibited a relatively constant water table approximately 65 cm below the ground surface (Figure 3a). Groundwater was recorded within 15 cm of the ground surface in the hillslope well, located 5 m upslope of the toe slope break, for the entire water year. Hillslope and riparian groundwater SC remained relatively constant throughout the year with a slight dilution during peak snowmelt (Figure 3a). Riparian groundwater SC dynamics at this transect always corresponded with those measured at the hillslope well.

[75] Transect 2 (T2) was located along a 7070 m^2, ~23° planar hillslope with a small 282 m^2 riparian area. The riparian buffer ratio at this site was 0.039. The riparian water table remained within 30 cm of the ground surface during the year and approached the surface when a hillslope water table occurred during snowmelt (Figure 3b). The transient hillslope water table first developed on 26 April 2007 and remained connected to the riparian zone through snowmelt until 11 June 2007 (46 day HRS connection). Initial riparian groundwater SC was 108 μS cm^{-1} and decreased to 29 μS cm^{-1} after a HRS water table connection was established (Figure 3b).

[76] Transect 3 (T3) was located near the base of a convergent hillslope hollow (~15.6°) with midrange UAA (10,165 m^2) and a large riparian area (1148 m^2). The riparian buffer ratio at this transect was 0.113. Riparian zone water tables remained within 20 cm of the ground surface for the entire year and surface saturation occurred during snowmelt and rain events (Figure 3c). A hillslope water table was first observed on 12 May 2006, exhibiting a rapid rise and sustained connection to its associated riparian zone (Figure 3c). Sustained HRS connectivity was observed during snowmelt (21 day connection) and the subsequent rain periods (8 day connection), totaling 29 days. Riparian groundwater before a hillslope water table initiation was 185 μS cm^{-1} but decreased to 77 μS cm^{-1} after a HRS connection was established (Figure 3c). Riparian groundwater SC never reached hillslope SC at this transect.

[77] Transect 4 (T4) was located along a ~26° divergent hillslope with small UAA (1527 m^2) and a large riparian area (700 m^2). The riparian buffer ratio at this site was 0.458. The riparian water table remained between 60 and 50 cm below the ground surface during base flow but increased to within 15 cm of the ground surface during snowmelt (Figure 3d). The hillslope water table response to rain and snow events was highly transient (Figure 3d) and early in the snowmelt period diurnal HRS water table connections/disconnections occurred in association with daily snowmelt peaks. HRS connectivity was observed for a total of 9 days at this transect. Riparian SC was 139 μS cm^{-1} before snowmelt and decreased to 70 μS cm^{-1} after a hillslope groundwater table developed (Figure 3d). The riparian groundwater SC never reached hillslope values at this transect.

[78] **Acknowledgments.** This work was made possible by NSF grant EAR-0337650 to McGlynn, EAR-0337781 to Gooseff, and an INRA fellowship awarded to Jencso. The authors appreciate extensive logistic collaboration with the U. S. Department of Agriculture, Forest Service, Rocky Mountain Research Station, especially, Ward McCaughey, Scientist-in-Charge of the Tenderfoot Creek Experimental Forest. We thank Jan Siebert, Thomas Grabs, and Robert Payn for technical and collaborative support and Galena Ackerman and John Mallard for performing laboratory analyses. We are grateful to Jennifer Jencso, Vince Pacific, Diego Riveros-Iregui, and especially Austin Allen for invaluable assistance in the field.

References

Ahmad, S., and S. I. Hasnain (2002), Hydrograph separation by measurement of electrical conductivity and discharge for meltwaters in the Ganga Headwater basin, Garhwal Himalaya, *J. Geol. Soc. India*, *59*(4), 323–329.

Allan, C. J., P. Vidon, and R. Lowrance (2008), Frontiers in riparian zone research in the 21st century, *Hydrol. Process.*, *22*, 3221–3222, doi:10.1002/hyp.7086.

Anderson, M. G., and T. P. Burt (1977), Automatic monitoring of soil moisture conditions in a hillslope spur and hollow, *J. Hydrol.*, *33*, 27–36.

Anderson, M. G., and T. P. Burt (1978), The role of topography in controlling throughflow generation, *Earth Surf. Processes Landforms*, *3*, 331–334.

Beven, K. J. (1978), The hydrological response of headwater and sideslope areas, *Hydrol. Sci. Bull.*, *23*, 419–437.

Boyer, E. W., G. M. Hornberger, K. E. Bencala, and D. M. McKnight (1997), Response characteristics of DOC flushing in an alpine catchment, *Hydrol. Processes*, *11*, 1635–1647.

Brinson, M. M. (1993), Changes in the functioning of wetlands along environmental gradients, *Wetlands*, *13*, 65–74.

Burns, D. A., P. S. Murdoch, G. B. Lawrence, and R. L. Michel (1998), Effect of groundwater springs on NO_3^- concentrations during summer in Catskill Mountain streams, *Water Resour. Res.*, *34*, 1987–1996, doi:10.1029/98WR01282.

Burns, D. A., J. J. McDonnell, R. P. Hooper, N. E. Peters, J. E. Freer, C. Kendall, and K. Beven (2001), Quantifying contributions to storm runoff through end-member mixing analysis and hydrologic measurements at the Panola Mountain Research Watershed (Georgia, USA), *Hydrol. Process.*, *15*, 1903–1924.

Burt, T. P., and B. P. Arkell (1987), Temporal and spatial patterns of nitrate losses from an agricultural catchment, *Soil Use Manage.*, *3*, 138–143.

Burt, T. P., and D. Butcher (1985), Topographic controls on soil moisture distribution, *J. Soil Sci.*, *36*, 469–476.

Burt, T. P., L. S. Matchett, K. W. T. Goulding, C. P. Webster, and N. E. Haycock (1999), Denitrification in riparian buffer zones: The role of floodplain hydrology, *Hydrol. Process.*, *13*, 1451–1463.

Burt, T. P., et al. (2002), Water table fluctuations in the riparian zone: comparative results from a pan-European experiment, *J. Hydrol.*, *265*(1–4), 129–148.

Buttle, J. M., P. J. Dillon, and G. R. Eerkes (2004), Hydrologic coupling of slopes, riparian zones and streams: An example from the Canadian Shield, *J. Hydrol.*, *287*, 161–177, doi:10.1016/j.jhydrol.2003.09.022.

Caissie, D., T. L. Pollock, and R. A. Cunjak (1996), Variation in stream water chemistry and hydrograph separation in a small drainage basin, *J. Hydrol.*, *178*, 137–157.

Carlyle, G. C., and A. R. Hill (2001), Groundwater phosphate dynamics in a river riparian zone: effects of hydrologic flow paths, lithology, and redox chemistry, *J. Hydrology*, *247*, 151–168.

Chanat, J., and G. M. Hornberger (2003), Modeling catchment-scale mixing in the near-stream zone: Implications for chemical and isotopic hydrograph separation, *Geophys. Res. Lett.*, *30*(2), 1091, doi:10.1029/2002GL016265.

Cirmo, C. P., and J. J. McDonnell (1997), Linking the hydrologic and biochemical controls of nitrogen transport in near-stream zones of temperate-forested catchments: A review, *J. Hydrol.*, *199*, 88–120.

Covino, T. P., and B. L. McGlynn (2007), Stream gains and losses across a mountain-to-valley transition: Impacts on watershed hydrology and stream water chemistry, *Water Resour. Res.*, *43*, W10431, doi:10.1029/2006WR005544.

Creed, I. F., and L. E. Band (1998), Export of nitrogen from catchments within a temperate forest: Evidence for a unifying mechanism regulated by variable source area dynamics, *Water Resour. Res.*, *34*, 3105–3120, doi:10.1029/98WR01924.

Devito, K., I. Creed, T. Gan, C. Mendoza, R. Petrone, U. Silins, and B. Smerdon (2005), A framework for broad-scale classification of hydrologic response units on the Boreal Plain: Is topography the last thing to consider?, *Hydrol. Process.*, *19*, 1705–1714, doi:10.1002/hyp.5881.

Dewalle, D. R., B. R. Swistock, and W. E. Sharpe (1988), 3-component tracer model for stormflow on a small Appalachian forested catchement, *J. Hydrol.*, *104*, 301–310.

Dunne, T., and R. D. Black (1970), Partial area contributions to storm runoff in a small New England watershed, *Water Resour. Res.*, *6*, 1296–1311, doi:10.1029/WR006i005p01296.

Duval, T. P., and A. R. Hill (2006), Influence of stream bank seepage during low-flow conditions on riparian zone hydrology, *Water Resour. Res.*, *42*, W10425, doi:10.1029/2006WR004861.

Farnes, P. E., R. C. Shearer, W. W. McCaughey, and K. J. Hansen (1995), Comparisons of Hydrology, Geology, and Physical Characteristics Between Tenderfoot Creek Experimental Forest (East Side) Montana, and Coram Experimental Forest (West Side) Montana, Final Report RJVA-INT-92734, USDA Forest Service, Intermountain Research Station, Forestry Sciences Laboratory. Bozeman, Mont., 19 pp.

Genereux, D. (1998), Quantifying uncertainty in tracer-based hydrograph separations, *Water Resour. Res.*, *34*, 915–919, doi:10.1029/98WR00010.

Grabs, T., K. J. Jencso, B. L. McGlynn, and J. Seibert (2010), Calculating terrain indices along streams—A new method for separating stream sides, *Water Resour. Res.*, doi:10.1029/2010WR009296, in press.

Grayson, R. B., A. W. Western, F. H. S. Chiew, and G. Blöschl (1997), Preferred states in spatial soil moisture patterns: Local and nonlocal controls, *Water Resour. Res.*, *33*, 2897–2908, doi:10.1029/97WR02174.

Hasnain, S. I., and R. J. Thayyen (1994), Hydrograph separation of bulk meltwaters of Dokriani-Bamak Glacier Basin, based on electrical-conductivity, *Curr. Sci.*, *67*, 189–193.

Hill, A. R. (1996), Nitrate removal in stream riparian zones, *J. Environ. Qual.*, *25*, 743–755.

Hill, A. R. (2000), Stream chemistry and riparian zones, in *Streams and Ground Waters*, edited by J. Jones and P. J. Mulholland, pp. 83–110, Academic Press, London.

Holdorf, H. D. (1981), Soil Resource Inventory of the Lewis and Clark National Forest, Interim. In-Service Report, on file with the Lewis and Clark National Forest, Forest Supervisor's Office, Great Falls, Mont.

Hooper, R., B. Aulenbach, D. Burns, J. J. McDonnell, J. Freer, C. Kendall, and K. Beven (1997), Riparian control of streamwater chemistry: Implications for hydrochemical basin models, *IAHS Redbook*, *248*, 451–458.

Huff, D. D., R. V. Oneill, W. R. Emanuel, J. W. Elwood, and J. D. Newbold (1982), Flow variability and hillslope hydrology, *Earth Surf. Proc. Land.*, *7*, 91–94.

Jencso, K. G., B. L. McGlynn, M. N. Gooseff, S. M. Wondzell, K. E. Bencala, and L. A. Marshall (2009), Hydrologic connectivity between landscapes and streams: Transferring reach- and plot-scale understanding to the catchment scale, *Water Resour. Res.*, *45*, W04428, doi:10.1029/2008WR007225.

Kobayashi, D. (1986), Separation of a snowmelt hydrograph by specific conductance, *J. Hydrol.*, *84*, 157–165.

Kobayashi, D., Y. Ishii, and Y. Kodama (1999), Stream temperature, specific cunductance and runoff process in mountain watersheds, *Hydrol. Process.*, *13*, 865–876.

Larkin, R., and J. Sharp (1992), On the relationship between river-basin geomorphology, aquifer hydraulics, and ground-water flow direction in alluvial aquifers, *Geol. Soc. Am. Bull.*, *104*, 1608–1620.

Laudon, H., and O. Slaymaker (1997), Hydrograph separation using stable isotopes, silica and electrical conductivity: An alpine example, *J. Hydrol.*, *201*, 82–101.

Lowrance, R. (1992), Groundwater nitrate and denitrification in a coastal plain riparian forest, *J. Environ. Qual.*, *21*, 401–405.

McDonnell, J. J., M. K. Stewart, and I. F. Owens (1991), Effect of catchment-scale subsurface mixing on stream isotopic response, *Water Resour. Res.*, *27*, 3065–3073, doi:10.1029/91WR02025.

McGlynn, B. L., J. J. McDonnell, J. B. Shanley, and C. Kendall (1999), Riparian zone flow path dynamics during snowmelt in a small headwater catchment, *J. Hydrol.*, *222*, 75–92.

McGlynn, B. L., and J. J. McDonnell (2003a), Role of discrete landscape units in controlling catchment dissolved organic carbon dynamics, *Water Resour. Res.*, *39*(4), 1090, doi:10.1029/2002WR001525.

McGlynn, B. L., and J. J. McDonnell (2003b), Quantifying the relative contributions of riparian and hillslope zones to catchment runoff, *Water Resour. Res.*, *39*(11), 1310, doi:10.1029/2003WR002091.

McGlynn, B. L., and J. Seibert (2003), Distributed assessment of contributing area and riparian buffering along stream networks, *Water Resour. Res.*, *39*(4), 1082, doi:10.1029/2002WR001521.

McGlynn, B. L., J. J. McDonnell, J. Seibert, and C. Kendall (2004), Scale effects on headwater catchment runoff timing, flow sources, and groundwater-streamflow relations, *Water Resour. Res.*, *40*, W07504, doi:10.1029/2003WR002494.

McGuire, K. J., J. J. McDonnell, M. Weiler, C. Kendall, B. L. McGlynn, J. M. Welker, and J. Seibert (2005), The role of topography on catchment-scale water residence time, *Water Resour. Res.*, *41*, W05002, doi:10.1029/2004WR003657.

Mulholland, P. J. (1992), Regulation of nutrient concentrations in a temperate forest streams: Roles of upland, riparian, and instream processes, *Limnol. Oceanogr.*, *37*, 1512–1526.

Ocampo, C. J., M. Sivapalan, and C. Oldham (2006), Hydrological connectivity of upland-riparian zones in agricultural catchments: Implications for runoff generation and nitrate transport, *J. Hydrol.*, *331*, 643–658, doi:10.1016/j.jhydrol.2006.06.010.

Pacific, V. J., K. G. Jencso, and B. L. McGlynn (2010), Variable flushing mechanisms and landscape structure control stream DOC export during snowmelt in a set of nested catchments, *Biogeochemistry*, *99*, 193–211, doi:10.1007/s10533-009-9401-1.

Payn, R. A., M. N. Gooseff, B. L. McGlynn, K. E. Bencala, and S. M. Wondzell (2009), Channel water balance and exchange with subsurface flow along a mountain headwater stream in Montana, United States, *Water Resour. Res.*, *45*, W11427, doi:10.1029/2008WR007644.

Peterjohn, W. T., and D. L. Correll (1984), Nutrient dynamics in an agricultural watershed—Observations on the role of a riparian forest, *Ecology*, *65*, 1466–1475.

Ramaswami, A., J. B. Milford, and M. J. Small (2005), *Integrated Environmental Modeling: Pollutant Transport, Fate, and Risk in the Environment*, 1st ed., 688 pp., Wiley.

Reynolds, M. (1995), Geology of Tenderfoot Creek Experimental Forest, Little Belt Mountains, Meagher County, Montana, in *Hydrologic and Geologic Characteristics of Tenderfoot Creek Experimental Forest, Montana*, *Final Rep. RJVA-INT-92734*, edited by P. Farnes, pp. 21–32, Intermt. Res. Stn., For. Serv., U.S. Dep. of Agric., Bozeman, Mont.

Scanlon, T. M., J. P. Raffensperger, and G. M. Hornberger (2001), Modeling transport of dissolved silica in a forested headwater catchment: Implications for defining the hydrochemical response of observed flow pathways, *Water Resour. Res.*, *37*, 1071–1082, doi:10.1029/2000WR900278.

Schlesinger, W. H. (1991), Biogeochemistry in freshwater wetlands and lakes, in *Biogeochemistry: An analysis of global change*, edited by W. H. Schlesinger, pp. 224–260, Academic Press, London.

Seibert, J., and B. L. McGlynn (2007), A new triangular multiple flow direction algorithm for computing upslope areas from gridded digital elevation models, *Water Resour. Res.*, *43*, W04501, doi:10.1029/2006WR005128.

Shaman, J., M. Stieglitz, and D. Burns (2004), Are big basins just the sum of small catchments?, *Hydrol. Processes*, *18*, 3195–3206, doi:10.1002/hyp.5739.

Sidle, R. C., Y. Tsuboyama, S. Noguchi, I. Hosoda, M. Fujieda, and T. Shimizu (2000), Stormflow generation in steep forested headwaters: A linked hydrogeomorphic paradigm, *Hydrol. Processes*, *14*, 369–385.

Sivapalan, M. (2003), Process complexity at hillslope scale, process simplicity at the watershed scale: is there a connection?, *Hydrol. Process.*, *17*(5), 1037–1041, doi:10.1002/hyp.5109.

Soulsby, C., P. J. Rodgers, J. Petry, D. M. Hannah, I. A. Malcolm, and S. M. Dunn (2004), Using tracers to upscale flow path understanding in mesoscale mountainous catchments: Two examples from Scotland, *J. Hydrol.*, *291*, 174–196, doi:10.1016/j.jhydrol.2003.12.042.

Soulsby, C., D. Tetzlaff, P. Rodgers, S. Dunn, and S. Waldron (2006), Runoff processes, stream water residence times and controlling landscape characteristics in a mesoscale catchment: An initial evaluation, *J. Hydrol.*, *325*, 197–221, doi:10.1016/j.jhydrol.2005.10.024.

Stewart, M., J. Cimino, and M. Ross (2007), Calibration of base flow separation methods with streamflow conductivity, *Ground Water*, *45*, 17–27, doi:10.1111/j.1745-6584.2006.00263.x.

Tetzlaff, D., J. Seibert, K. J. McGuire, H. Laudon, D. A. Burn, S. M. Dunn, and C. Soulsby (2009), How does landscape structure influence catchment transit time across different geomorphic provinces?, *Hydrol. Processes*, *23*, 945–953, doi:10.1002/hyp.7240.

Uchida, T., Y. Asano, Y. Onda, and S. Miyata (2005), Are headwaters just the sum of hillslopes?, *Hydrol. Processes*, *19*, 3251–3261, doi:10.1002/hyp.6004.

Vidon, P., and A. R. Hill (2004a), Denitrification and patterns of electron donors and acceptors in eight riparian zones with contrasting hydrogeology, *Biogeochemistry*, *71*, 259–283.

Vidon, P., and A. Smith (2007), Upland controls on the hydrological functioning of riparian zones in glacial till valleys of the midwest, *J. Am. Water Resour. Assoc.*, *43*, 1524–1539.

Vidon, P. G. F., and A. R. Hill (2004b), Landscape controls on nitrate removal in stream riparian zones, *Water Resour. Res.*, *40*, W03201, doi:10.1029/2003WR002473.

Welsch, D. L., C. N. Kroll, J. J. McDonnell, and D. A. Burns (2001), Topographic controls on the chemistry of subsurface stormflow, *Hydrol. Processes*, *15*, 1925–1938.

Weyman, D. R. (1970), Throughflow on hillslopes and its relation to the stream hydrograph, *Bull. Int. Assoc. Scientific Hydrol.*, *15*, 25–33.

Wolock, D. M., J. Fan, and G. B. Lawrence (1997), Effects of basin size on low-flow stream chemistry and subsurface contact time in the Neversink River Watershed, New York, *Hydrol. Process.*, *11*, 1273–1286.

K. E. Bencala, U.S. Geological Survey, 345 Middlefield Road, Menlo Park, CA 94025, USA.

M. N. Gooseff, Civil Environmental Engineering Department, Penn State University, 212 Sackett Bldg., University Park, PA 16802, USA.

K. G. Jencso and B. L. McGlynn, Department of Land Resources and Environmental Sciences, Montana State University, Bozeman, MT 59717, USA. (kelseyjencso@gmail.com)

S. M. Wondzell, U.S. Forest Service, Pacific Northwest Research Station Olympia Forestry Sciences Lab, Olympia, WA 98512, USA.